Difference-frequency ultrasound generation from microbubbles under dual-frequency excitation*

Ma Qing-Yu(马青玉)[a], Qiu Yuan-Yuan(邱媛媛)[b], Huang Bei(黄 蓓)[b], Zhang Dong(章 东)[b]†, and Gong Xiu-Fen(龚秀芬)[b]

[a] School of Physics and Technology, Nanjing Normal University, Nanjing 210097, China
[b] Key Laboratory of Modern Acoustics, Ministry of Education, Institute of Acoustics, Nanjing University, Nanjing 210093, China

(Received 24 November 2009; revised manuscript received 28 March 2010)

The difference-frequency (DF) ultrasound generated by using parametric effect promises to improve detection depth owing to its low attenuation, which is beneficial for deep tissue imaging. With ultrasound contrast agents infusion, the harmonic components scattered from the microbubbles, including DF, can be generated due to the nonlinear vibration. A theoretical study on the DF generation from microbubbles under the dual-frequency excitation is proposed in formula based on the solution of the RPNNP equation. The optimisation of the DF generation is discussed associated with the applied acoustic pressure, frequency, and the microbubble size. Experiments are performed to validate the theoretical predictions by using a dual-frequency signal to excite microbubbles. Both the numerical and experimental results demonstrate that the optimised DF ultrasound can be achieved as the difference frequency is close to the resonance frequency of the microbubble and improve the contrast-to-tissue ratio in imaging.

Keywords: difference-frequency, microbubble, dual-frequency excitation, parametric effect
PACC: 4335, 8750C

1. Introduction

Ultrasound at lower frequency is beneficial for imaging deep tissues owing to its lower attenuation, but it is still limited by the lower spatial resolution.[1] Since Westervelt first put forward the theory of parametric array,[2] the difference-frequency (DF) technique has been widely utilised in many medical applications. Gong *et al.*[3] carried out the computed tomography (CT) of the acoustic nonlinearity parameter B/A for biological tissues using the DF technique. Chiou *et al.*[4] concluded that the differential tissue harmonic imaging performs better than the fundamental imaging with regard to detail resolution, and shows deeper penetration depth over tissue harmonic imaging. The low frequency DF even to 20 kHz was selected to increase the penetration depth for tissue imaging using the vibro-acoustic spectrography technique[5] and the elasticity imaging[6] technique. However, the amplitude of the DF ultrasound is about 60 dB lower than that of the primary waves in biological tissues.[7] It is required to obtain the DF ultrasound with acceptable signal-noise ratio (SNR) for tissue imaging.

The introduction of ultrasound contrast agents (UCAs) increases the diagnostic capabilities of ultrasound imaging.[8−12] The unique echo properties of the microbubbles[13,14] enable ultrasound contrast imaging to be implemented not only in linear mode, but also in nonlinear modes.[15−17] When microbubbles are present, the generated DF ultrasound can be greatly enhanced owing to the great nonlinearity of the microbubbles. In addition, the DF ultrasound scattered from the microbubbles is distinctly greater than that from the surrounding tissues. Combining the DF technique with the UCAs, Newhouse and Shankar developed a dual-frequency excitation technique for bubble size estimation.[18−20] Wu and Tsao put forward the ultrasonic short-pulse response approximation of microbubbles and provided the special bandwidth dependent property and potential applications in tissue imaging.[21,22]

In this study, the DF ultrasound generation from microbubbles under dual-frequency excitation is theoretically and experimentally investigated. Based on the modified Raleigh–Plesset–Noltingk–Neppiras–

*Project supported by the National Natural Science Foundation of China (Grant Nos. 10974098 and 10774071), the Natural Science Foundation of Jiangsu Province, China (Grant No. BK2009407), the Doctoral Foundation of Ministry of Education of China (Grant No. 20093207120003), and the National Basic Research Program of China (Grant No. 2010CB732600).
†Corresponding author. E-mail: dzhang@nju.edu.cn
© 2010 Chinese Physical Society and IOP Publishing Ltd

Porirsky (RPNNP) differential equation,[23] the dynamic behaviour at the DF is theoretically discussed with respect to acoustic intensity, incident frequencies of the two primary waves as well as the bubble size. Experiments for the DF ultrasound generation are performed to verify the theoretical prediction. Furthermore, the optimisation of the DF generation from microbubbles is summarized as the basis for the further study on the contrast DF ultrasound imaging.

2. Principle and method

2.1. Theory

When a microbubble is insonated by ultrasound, the modified RPNNP equation[23] in volume pulsation can be simplified by neglecting the energy dissipation of the acoustic heating and the thermal conduction.

$$\rho R R'' + \frac{3}{2}\rho (R')^2 = \left(p_0 + \frac{2\sigma}{R_0}\right)\left(\left(\frac{R_0}{R}\right)^{3\gamma} - 1\right) - 4\mu\frac{R'}{R} + p_{\rm ext}(t), \quad (1)$$

where ρ is the density of the liquid, γ is the polytropic exponent, R and R_0 are the instantaneous and initial radii of the bubble, R' and R'' are the first and second order derivatives of the instantaneous radius respectively; p_0 is the ambient pressure as a constant and $p_{\rm ext}$ is the external driving acoustic pressure. The mass and heat transfers between the bubble and the liquid are neglected and the fluid is assumed to be Newtonian with surface tension coefficient σ and shear viscosity μ. As described by de Jong, the bubble resonance frequency (BRF)[24] of an encapsulated bubble is

$$f_0 = \frac{1}{2\pi R_0}\sqrt{\frac{3\gamma p_0}{\rho}\left(p_0 + \frac{\pi}{3}\frac{S_{\rm e}}{\gamma R_0}\right)},$$

where $S_{\rm e}$ is the elastic parameter of the shell of the bubble.

With the assumption of small radial vibration of the bubble under the low external driving acoustic pressure, Eq. (1) can be rewritten as

$$\rho R_0^2(1+x)x'' + \frac{3}{2}\rho R_0^2 (x')^2 = \left(p_0 + \frac{2\sigma}{R_0}\right)\left(1 - 3\gamma x + \frac{3\gamma(3\gamma+1)}{2}x^2\right) - \left(p_0 + \frac{2\sigma}{R_0}(1 - x + x^2)\right) - 4\mu(1-x)x' + p_{\rm ext}(t), \quad (2)$$

where the instantaneous radius of the bubble is expressed as $R = R_0(1+x)$ for $x << 1$ of the small amplitude vibration.

When a dual-frequency signal containing two frequencies (f_1 and f_2) with acoustic pressures p_1 and p_2 is used to excite the transducer, the produced acoustic pressure can be expressed as $p_{\rm ext}(t) = p_1\cos(2\pi f_1 t + \theta_1) + p_2\cos(2\pi f_2 t + \theta_2)$. The centre frequency is defined as $f_{\rm c} = (f_1 + f_2)/2$ and the DF is $\Delta f = f_1 - f_2$. The time duration of the pulse is set to $T = 1/\Delta f$ to cover Δf for the spectrum analyses, and the initial phase difference $\Delta\theta = \theta_1 - \theta_2$ can be varied from 0 to 2π. Owing to the parametric effect, the nonlinear components are generated including the harmonics, the sum- and the difference-frequency components. The scattered signal from the bubble can be written as

$$A(t) = A_0 + A_1\cos(2\pi f_1 t + \phi_1) + A_2\cos(2\pi f_2 t + \phi_2) + A_3\cos(2\pi f_3 t + \phi_3) + A_4\cos(2\pi f_4 t + \phi_4) + A_{\rm s}\cos(2\pi f_{\rm s} t + \phi_{\rm s}) + A_{\rm d}\cos(2\pi f_{\rm d} t + \phi_{\rm d}) + \ldots, \quad (3)$$

where A_0, A_1, A_2, A_3 and A_4 are the amplitudes of the direct current signal, the fundamentals and the second harmonics; $f_3 = 2f_1$ and $f_4 = 2f_2$ represent the second harmonics; $A_{\rm s}$ and $A_{\rm d}$ are the amplitudes at the sum- and difference-frequencies of $f_{\rm s} = f_1 + f_2$ and $f_{\rm d} = f_1 - f_2$, respectively. For simplicity, we ignore the high order modulations. The amplitudes at f_1 and f_2 are given as:[21,22]

$$A_m = \frac{p_m X_m}{4\pi^2\rho f_0^2 R_0^2}, \quad m = 1, 2, \quad (4)$$

where $X_m = [(1-\Omega_m)^2 + \delta^2\Omega_m^2]^{-1/2}$, $\Omega_{1,2} = (f_{\rm c} \pm \Delta f/2)/f_0$ and $\delta = 4\mu/(2\pi\rho f_0^2 R_0^2)$. The amplitude at the DF can be expressed as

$$A_{\rm d} = A_1 A_2 X'_{12} Y'_{12}, \quad (5)$$

where

$$Y'_{12} = \{[(\Omega_1^2 + \Omega_2^2)/2 + 3\Omega_1\Omega_2/2 + K]^2 + \delta^2 \Omega'^2_{12}/4\}^{1/2},$$

$$X'_{12} = [(1 - \Omega'^2_{12})^2 + \delta^2 \Omega'^2_{12}]^{-1/2},$$

$$K = \left[3\gamma(3\gamma+1)\left(p_0 + \frac{2\sigma}{R_0}\right) - \frac{4\sigma}{R_0}\right]/8\pi^2\rho R_0^2 f_0^2$$

and $\Omega'_{12} = \Delta f / f_0$.

Supposing that the amplitudes of two primary waves are equal ($p = p_1 = p_2$), and that the equivalent fractional bandwidth $Be = \Delta f / f_c$ is small enough, we have $A_1 \approx A_2$. The amplitude of the DF component can be simplified to

$$A_d \approx \frac{p^2 X_1^2 X'_{12} Y'_{12}}{(4\pi^2 \rho f_0^2 R_0^2)^2}. \quad (6)$$

It is obvious that the amplitude of the DF component is dependent on the square of the peak pressure of the incident primary wave and the properties of the bubble.

2.2. Microbubble preparation and experimental setup

The microbubbles used in this study are developed in our laboratory, the detailed process of the preparation can be found in the previous study.[10−15] In the measurement, the solution is further diluted to a concentration of bubbles at about 2.0×10^6 bubbles/mL. The size distribution of the microbubble suspension is measured by the particle size analyser (Mastersizer 2000, Malvern Instruments INC, UK) and presented in Fig. 1. It is clearly found that the bubble diameters mainly range from 1 to 10 μm and the corresponding BRF is from about 3 to 0.3 MHz.

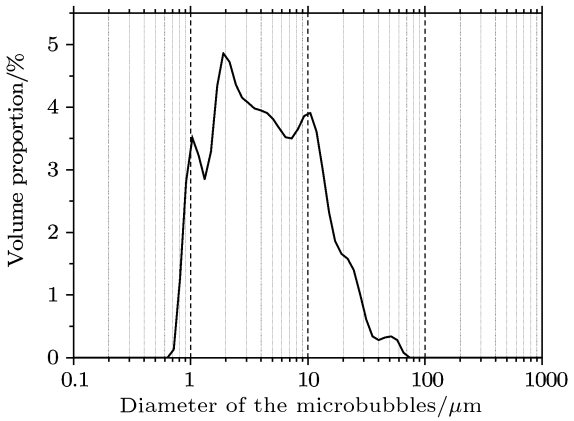


Fig. 1. Size distribution of the microbubble suspension.

Figure 2 provides the schematic illustration of the experimental setup for measuring the DF ultrasound generated from the microbubbles. A dual-frequency tone burst signal of the central frequency 6 MHz and the frequency difference Δf is generated by a programmable function generator (Agilent 33250A, Loveland, CO, USA) at a pulse repetition frequency of 1 kHz. The signal is amplified by a 55 dB broadband power amplifier (ENI A150, Rochester, NY, USA) to excite a planar piezoelectric transducer (central frequency=6 MHz, diameter=14 mm, Panametrics V301, USA). The acoustic signal is detected by a calibrated needle broadband hydrophone (TNU0001A, NTR, USA) with an active diameter of 0.6 mm and an upper frequency limit of 20 MHz. The received signals are amplified by a low-noise 30 dB preamplifier (HPA30, NTR, USA) and acquired using a digital oscilloscope (Agilent 54830, USA). The digitised signals are saved and further processed using the fast Fourier transform (FFT) algorithm spectrum analysis in the computer. Both the transmitter and the receiver are immersed into distilled water with a distance of 60 mm. The sample container is a Plexiglas cylinder (radius x height = 2 cm × 2 cm) with two parallel windows covered by thin sound-permeable membranes. A linear 3-axial scan system (Newport ESP7000, USA) controlled by a PC via Labview software (NI Corp., TX, USA) is used for aligning the transmitter and receiver. All measurements are performed at room temperature (approximately 22 °C).

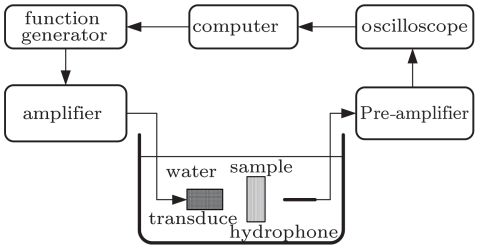


Fig. 2. Block diagram of the experimental setup.

3. Results

Figure 3 shows the theoretical and experimental spectra of scattered signals from microbubbles excited by a dual-frequency signal (f_1 = 5.5 MHz, f_2 = 6.5 MHz, Δf = 1 MHz, $\theta_1 = \theta_2 = 0$) at the acoustic pressure of 0.5 MPa, where Fig. 3(a) is calculated from Eq. (1). In the numerical calculation, parameters of the microbubble are: R_0 = 3 μm, $p_0 = 1.01 \times 10^5$ Pa, ρ = 998 kg·m^{-3}, γ = 1.07, μ = 0.01 Pa·s, σ = 0.051 N·m^{-1} and c_0 = 1540 m/s. In Fig. 3(a), the fundamental frequencies (5.5 and

6.5 MHz), the second harmonics (11 and 13 MHz), and the DF (1 MHz) are observed in the spectrum. Furthermore, the high order modulated frequencies of 4.5, 7.5 and 12 MHz as well as 16.5, 17.5, 18.5 and 19.5 MHz can also be found in this figure owing to the nonlinearity of the microbubble. The experimental results in Figs. 3(b) and 3(c) show a comparison before and after the microbubbles perfusion and confirm the predicted results. In Fig. 3(b), the magnitudes at the two fundamental frequencies are about 16 and 22 dB, but the magnitude at the DF of 1 MHz is about 40 dB lower because of the low nonlinearity in water. In addition, the noise level of the experimental system is obviously found, such as the peak at 0.6 MHz. When the microbubbles are present, the magnitudes at the fundamental frequencies are reduced by about 13 dB owing to high attenuation of the microbubbles and the energy transfer of the frequency modulations as shown in Fig. 3(c). The magnitudes of the DF at 1 MHz is enhanced by about 28 dB because of the bubble resonance.

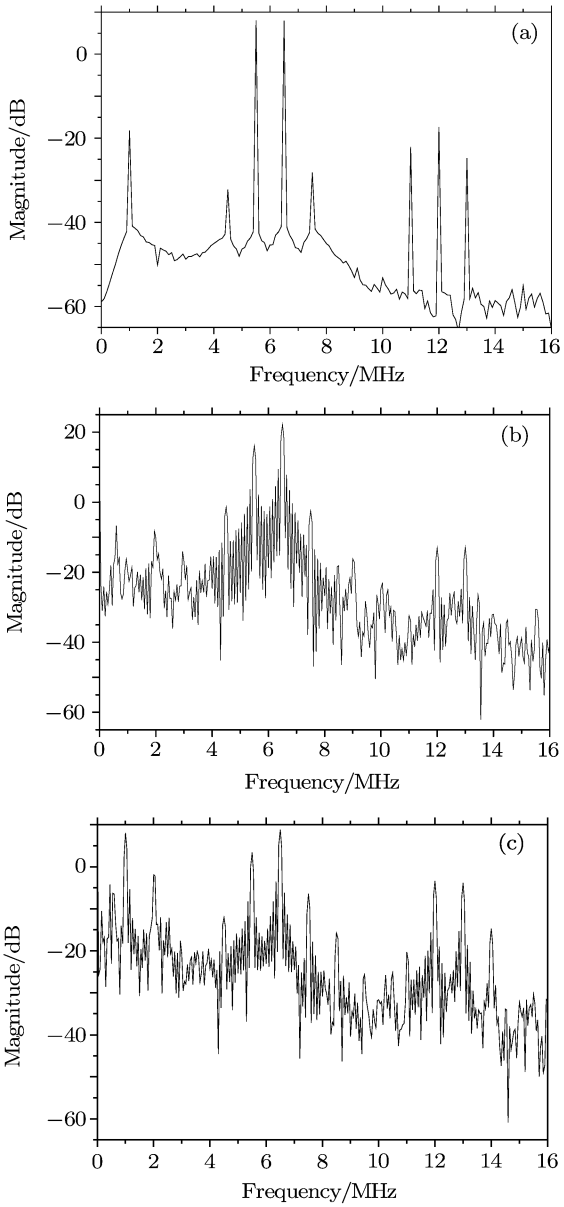


Fig. 3. Theoretical (a) and experimental spectra of the scattered signal before (b) and after (c) the microbubbles perfusion.

By changing the incident acoustic pressure from 0.1 to 1.4 MPa, the measured pressure dependence of the DF component generated from the microbubbles is shown in Fig. 4 as the rectangle points. For comparison, the theoretical results are also provided in this figure as the solid line based on Eq. (2). In addition, the experimental results at the fundamental frequency are also presented as the triangle points. The experimental results coincide well with the theoretical predictions. When the incident acoustic pressure is below 0.6 MPa, the amplitude of DF is proportional to the squared source pressure while the amplitude at the fundamental frequency is proportional to the source pressure, which is in agreement with Eqs. (4) and (5) basically. Further increasing the source pressure to 1 MPa, the amplitude of the DF component still enhances but with the reduced growth rate. It suggests that the applied source pressure is beyond the scope of small amplitude vibration. The DF ultrasound reaches its maximal value when the source pressure is about 1 MPa, then decreases at the higher acoustic pressures due to the intensive vibration and even the microbubble destruction.

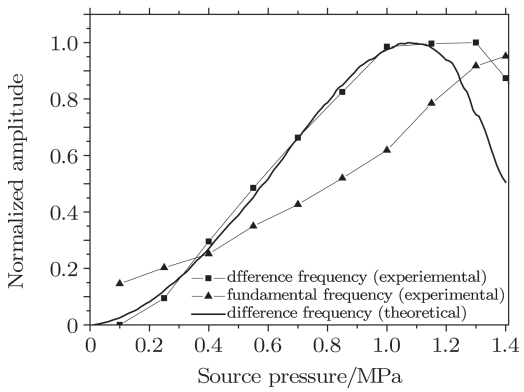


Fig. 4. Pressure dependences of the components at the DF and fundamental frequencies.

By keeping the central frequency of 6 MHz and the acoustic pressure of 0.5 MPa, we change the frequency difference of the two incident frequencies from 0.25 MHz to 3 MHz. The curve of the amplitudes of the generated DF ultrasound versus frequency difference is plotted as solid circles in Fig. 5, which are

normalised by the maximal value. For comparison, the corresponding theoretical predicted curve is also plotted as open triangles in this figure. Both the measured and theoretical results demonstrate that the DF ultrasound reaches its peak as the frequency difference is close to the bubble resonant frequency. The discrepancy between the theoretical prediction and the measurement comes from the fact that the microbubbles in the measurement have the bubble size distribution while the theoretical results are calculated from a single bubble.

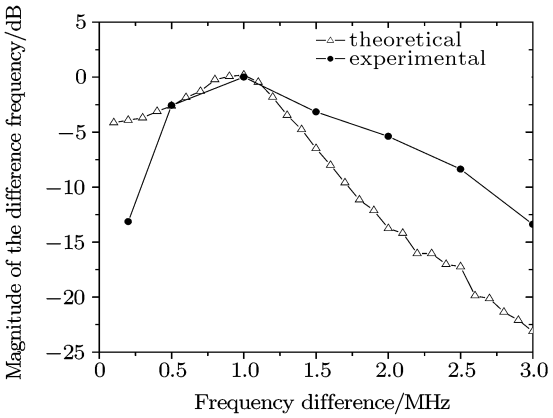


Fig. 5. Frequency difference dependence of the DF generation.

4. Discussion and conclusion

As indicated by the simulations and measurements, the DF ultrasound generation from microbubbles is dependent on the peak acoustic pressure and the frequency difference of the two incident frequencies as well as the resonance frequency of microbubbles. To decrease the frequency aliasing of the received signal, the resonance frequency f_0 of the microbubble should be far away from the centre frequency f_c of the transmitted signal. On the other hand, the two frequencies of the dual-frequency excitation should be close enough to generate a low frequency signal, and an suitable frequency difference should be chosen to satisfy $\Delta f \approx f_0$.

It should be noted that our theoretical study is based on the RPNNP equation for a single microbubble. However, mostly UCAs have a size distribution, which produces a resonant frequency distribution. For the multi-bubble system, there exists vibration interaction among the bubbles in the practical measurement, leading to the complex frequency modulation and vibration superposition for the transducer detection.

In conclusion, we have proposed a theoretical investigation on the mechanism of the DF generation under dual-frequency excitation in order to increase the acoustic penetration depth with the improved SNR in acoustic imaging in this paper. Based on the nonlinear dynamics of microbubbles, the DF generation is theoretically analysed. The optimisation of the DF generation is discussed with respect to the incident acoustic pressure, frequency, and the microbubble size. It is concluded that there is an obvious amplitude peak when the microbubble resonance frequency f_0 is close to the frequency difference Δf of the incident frequencies. Measurements of the DF generation were also performed by using a dual-frequency signal to excite our self-developed microbubble suspension. The measured results qualitatively validated our theoretical predictions. Even though the experimental study on the microbubbles at a lower resonant frequency is required for further investigation, this preliminary study suggests the potential application for the contrast difference frequency imaging in deep tissue imaging to improve the SNR and the contrast-to-tissue ratio.

References

[1] Wells P N T 2006 *Phys. Med. Biol.* **51** R83

[2] Westervelt P J 1975 *J. Acoust. Soc. Am.* **29** 199

[3] Gong X F, Zhang D, Liu J H, Wang H L, Yan Y S and Xu X C 2004 *J. Acoust. Soc. Am.* **116** 1819

[4] Chiou S Y, Forsberg F, Fox T B and Needleman L 2007 *J. Ultrasound Med.* **26** 1557

[5] Fatemi M and Greenleaf J F 1998 *Science* **280** 82

[6] Erpelding T N, Hollman K W and O'Donnell M 2005 *IEEE Trans. Ultrason. Ferr. Freq. Contr.* **52** 971

[7] Wang H L, Zhu X F, Gong X F and Zhang D 2003 *Chin. Sci. Bull.* **48** 2427

[8] Ophir J and Parker J P 1989 *Ultrasound Med. Biol.* **15** 319

[9] de Jong N, Cornet R and Lancee C T 1994 *Ultrasonics* **32** 447

[10] Gong Y J, Zhang D, Gong X F, Tan K B and Liu Z 2006 *Chin. Phys.* **15** 1526

[11] Fan T B, Zhang D, Zhang Z, Ma Y and Gong X F 2008 *Chin. Phys.* B **17** 3372
[12] Liu Z B, Fan T B, Zhang D and Gong X F 2009 *Chin. Phys.* B **18** 4932
[13] Zhang D, Gong Y J and Gong X F 2007 *Phys. Med. Biol.* **52** 5531
[14] Gong Y J, Zhang D, Xi X Y Gong X F and Liu Z 2007 *Acta Phys. Sin.* **56** 7051 (in Chinese)
[15] Liang B, Zhu Z M and Cheng J C 2006 *Chin. Phys.* **15** 412
[16] Wang W L and Zhang B X 2008 *Acta Phys. Sin.* **57** 3613 (in Chinese)
[17] Qian Z W and Xiao L 2008 *Chin. Phys.* B **17** 3785
[18] Phelps A D and Leighton T G 1996 *J. Acoust. Soc. Am.* **99** 1985
[19] Newhouse V L and Shankar P M 1984 *J. Acoust. Soc. Am.* **75** 1473
[20] Wyczalkowski M and Szeri A J 2003 *J. Acoust. Soc. Am.* **113** 3073
[21] Wu C Y and Tsao J 2003 *J. Acoust. Soc. Am.* **113** 2662
[22] Wu C Y, Tsao J and Chou Y H 2005 *Ultrasound Med. Biol.* **31** 1199
[23] Prosperetti A 1982 *Phys. Fluids* **25** 409
[24] Church C C 1995 *J. Acoust. Soc. Am.* **97** 1510